Distribution Agreement

In presenting this thesis as a partial fulfillment of the requirements for a degree from Emory University, I hereby grant to Emory University and its agents the non-exclusive license to archive, make accessible, and display my thesis in whole or in part in all forms of media, now or hereafter now, including display on the World Wide Web. I understand that I may select some access restrictions as part of the online submission of this thesis. I retain all ownership rights to the copyright of the thesis. I also retain the right to use in future works (such as articles or books) all or part of this thesis.

Lucky Khambouneheuang April 5, 2016

Mechanosensitive miRNA targets TIMP3 to increase matrix degradation in the aortic valve endothelium

by

Lucky Khambouneheuang

Dr. Hanjoong Jo
Adviser

Department of Biology

Dr. Hanjoong Jo

Adviser

Dr. Arri Eisen

Committee Member

Dr. Cory Labrecque

Committee Member

2016

Mechanosensitive miRNA targets TIMP3 to increase matrix degradation in the aortic valve endothelium

By

Lucky Khambouneheuang

Dr. Hanjoong Jo

Adviser

An abstract of
a thesis submitted to the Faculty of Emory College of Arts and Sciences
of Emory University in partial fulfillment
of the requirements of the degree of
Bachelor of Sciences with Honors

Department of Biology

2016

Abstract

Mechanosensitive miRNA targets TIMP3 to increase matrix degradation in the aortic valve endothelium

By Lucky Khambouneheuang

Heart disease, including calcified aortic valve disease (CAVD), remains the leading cause of death worldwide. The role of endothelial cells (ECs) in CAVD remains relatively unknown; however, disease develops in a side-dependent manner. Preferentially, calcification occurs on the fibrosa endothelium, which is subjected to disturbed blood flow, whereas the ventricularis endothelium, which is subjected to stable blood flow, is relatively unaffected. Our research goal is to discover mechanisms, especially a new type of small molecules (known as microRNAs) by which mechanical force regulates endothelial inflammation and the resulting aortic valve (AV) calcification. We hypothesize that miRNA181b is upregulated by disturbed flow at the AV fibrosa endothelium, leading to decreased expression of TIMP3 and increased matrix degradation. Several microRNAs (miRNAs) have been shown to be mechanosensitive (flow-sensitive), and thus may play a role in the development of AV calcification. Using human aortic valve endothelial cells (HAVECs) in our in vitro cone-and-plate system that simulates different blood flow conditions, laminar shear (LS) versus oscillatory shear (OS), we have found several miRNAs that are regulated by flow, including miRNA-181b. Compared to HAVECs subjected to LS, HAVECs in OS demonstrated significant upregulation in miRNA-181a and -181b expression. Using miRTarBase, we further identified and studied miRNA-181b targets, including genes GATA6, SIRT1, and TIMP3. We also found significantly decreased GATA6, SIRT1, and TIMP3 expression in HAVECs subjected to OS stress. Moreover, our gelatinase assay significantly confirmed increased MMP activity and extracellular matrix degradation in HAVECs subjected to OS. We further transfected HAVECs with pre- and anti-miRNA-181b to study the direct relationship between miRNA-181b and TIMP3. For pre-miRNA-181b treated samples, we observed significant decrease in expression for GATA6, SIRT1, and TIMP3 in HAVEC in OS. For anti-miRNA-181b treated HAVECs, we observed significant decreased MMP activity compared to control samples. Our study overall correlatively demonstrates that in ECs subjected to OS, miRNA-181b is upregulated, leading to the decrease expression of TIMP3 and increased ECM degradation. In the future, our ongoing work may provide insight into novel therapeutic treatments targeting specific mechanosensitive miRNAs to treat AV stenosis and disease.

Mechanosensitive miRNA targets TIMP3 to increase matrix degradation in the aortic valve endothelium

By

Lucky Khambouneheuang

Dr. Hanjoong Jo

Adviser

A thesis submitted to the Faculty of Emory College of Arts and Sciences
of Emory University in partial fulfillment
of the requirements of the degree of
Bachelor of Sciences with Honors

Department of Biology

2016

Acknowledgements

This work was supported by a program project grant to Dr. Jo from NHLBI, as well as other NIH grants. My deepest thank to Dr. Jo for welcoming me to his lab and to Jack Heath for being an incredible mentor during my time as a Petit researcher. I especially want to thank Jack for his incredible support and guidance throughout my time at Emory. I will cherish all the lessons you have instilled in me, as I continue to pursue a career in the science. Secondly, I would like to extend my sincerest gratitude to Drs. Eisen and Labrecque. Thank you for supporting me not only in the Honors program but also in life with your wisdom and unconditional support. I am truly grateful for everyone who has helped me accomplished this project and rewarding experience.

Table of Contents

List of Symbols and Abbreviations

AV	aortic valve
BCL2	B-cell lymphoma 2
CAVD	calcific aortic valve disease
CDX2	caudal type homeobox 2
EC	endothelial cells
ECM	extracellular matrix
F	fibrosa
GAG	glycosaminoglycan
GATA6	GATA-binding protein 6
HAVEC	human aortic valve endothelial cell
ICAM	intercellular adhesion molecule
LS	laminar shear
miRNA	microRNA
MMP	matrix metallopeptidase
NLK	nemo-like kinase
OS	oscillatory shear
PCR	polymerase chain reaction
RISC	RNA-induced silencing complex
SIRT1	sirtuin-1
TIMP3	tissue inhibitor of metallopeptidase 3
V	ventricularis
VCAM	vascular cell adhesion molecule
VEC	valvular endothelial cell
vHAVEC	ventricularis human aortic valve endothelial cell
VIC	valvular interstitial cell

List of Figures

List of Tables

Introduction

1.1 Clinical Significance of Calcific Aortic Valve Disease

Heart disease, including calcific aortic valve disease (CAVD), remains the leading cause of death worldwide. Viewed for many years as a "wear and tear" process (1), CAVD is an age-related, degenerative disorder; its prevalence in the elderly population increases with advancing age (2). Currently, CAVD affects 25-29% of people over 65 years of age and 48% of people older than 84 (3-7). Clinically, valvular diseases are often associated with and/or considered progressive hallmarks of other detrimental cardiovascular events, including atherosclerosis, myocardial infarction, angina, congestive heart failure, and stroke (6,8). Globally, cardiovascular disease accounts for 17.3 million deaths per year, and this number is expected to rise to approximately 24 million by 2030 (9).

CAVD is a slowly progressive disorder with a disease continuum that ranges from aortic sclerosis, the mild thickening of the valve with no blood outflow obstruction, to aortic stenosis, the severe calcification of the valve with motion impairment in the leaflet (3,10). These disease processes are often associated with the negative outcomes of various cardiovascular disorders. In the Cardiovascular Health Study, a prospective study of about 5,600 men and women 65 years of age or older, aortic stenosis was associated with an 50% increased risk of death from cardiovascular causes and of myocardial infarction, even in absence of significant obstruction in the left ventricular outflow (6). Unfortunately, there are currently no effective pharmacological therapies available for affected patients. Prosthetic valve replacement and/or repair surgeries are the only treatment options for CAVD. Within the United States, approximately 98,000 aortic valve replacements are performed annually for severe aortic stenosis (11). Without surgical treatment, patients with this disease have a 50% chance of living two years and 20% chance of

living for five years after symptom onset (12). These statistics highlight CAVD prevalence, particularly in the elderly population, and the need for a clearer understanding of the disease pathways, enabling earlier drug therapy or intervention in CAVD.

1.2 Aortic Valve Structure, Cellular Components, and Functions

The aortic valve (AV) acts to regulate unidirectional blood flow from the left ventricle to the aorta and systemic vasculature (13). The AV is stratified into three layers: the fibrosa, facing the aorta; the ventricularis, facing the left ventricle; and the spongiosa, which is located between the fibrosa and ventricularis (Figure 1).

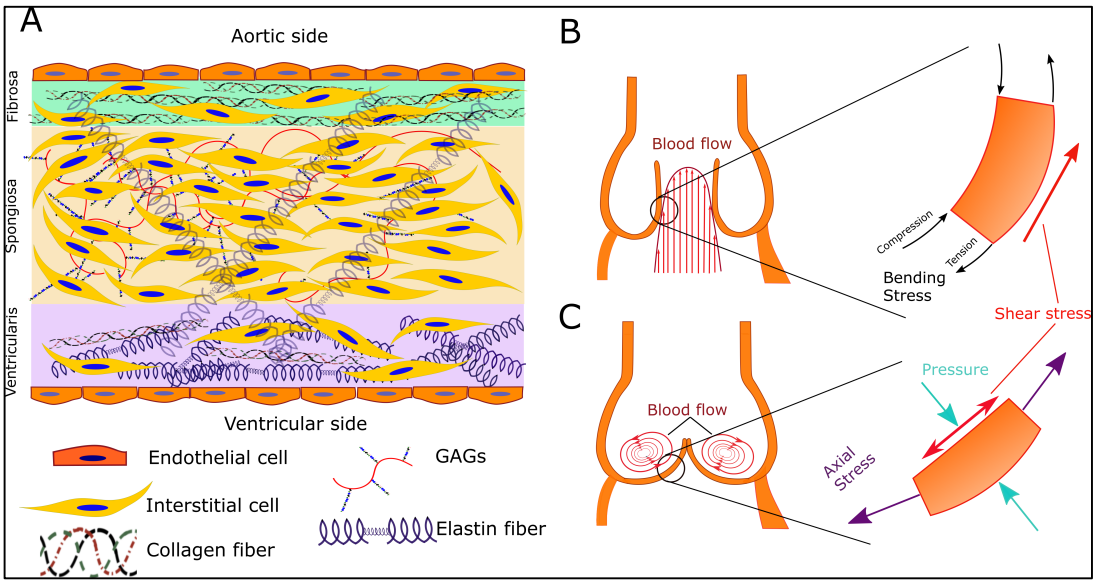

Figure 1. Aortic valve structure and function. (A) The AV is comprised of three layers: the fibrosa, facing the aorta; ventricularis, facing the ventricle; and the spongiosa, which is located between the fibrosa and ventricularis. The AV is also comprised of two main cell types: endothelial cells and interstitial cells. Endothelial cells line the AV, whereas the interstitial cells are found throughout the structure. Also, collagen and elastin fibers are found in all three layers; glycosaminoglycans (GAGs) are only found in the spongiosa layer. (B) The ventricularis is subjected to stable, laminar shear stress due to blood ejection from the left ventricle during systole (C). The fibrosa is subjected to random, oscillatory shear stress due to blood flow. Modified from (14).

Each layer is comprised of differing amounts of collagen, elastin, and glycosaminoglycans. The fibrosa is primarily composed of circumferentially oriented collagen fibers and fibroblasts and functions as the main load-bearing layer. The ventricularis consists of a network of collagen and radially aligned elastin fibers (6,10,15); their structural network enables reduced radial strain when the valve is fully opened and also aids the valve leaflet with recoil to its undeformed resting state (15,16). In the middle, the spongiosa is a layer of proteoglycans and scattered collagen fiber that serves to link and lubricate the fibrosa and ventricularis, which are constantly subjected to shear stress, hemodynamic friction, and pressurization (6,10,15). In concert, these three layers work to provide structural integrity and tensile strength within the AV for decades of repetitive motion in the cardiac cycle, opening and closing approximately 3 billion times within the average human lifespan (16).

Additionally, the AV is comprised of two cell types: the valvular interstitial cells (VICs) and valvular endothelial cells (VECs). Both VICs and VECs are important for maintaining tissue homeostasis of the AV via biochemical secretion, matrix proteins, and matrix-modeling enzymes (17). The VICs are most prevalent in the heart valves and comprise of a mix of heterogeneous cells that express differing phenotypes, such as those of myofibroblasts, osteoblasts, fibroblasts, and smooth muscle cells (18). Based on previous studies, VICs play an important role in the normal functioning valve and the progression of AV diseases (19). Particularly, in the progression of AV calcification, VICs differentiate into osteoblast-like cells, a process involving mediators such as bone morphogenetic proteins and the TGF-β pathway (20). Osteoblast-like VICs also deposit fibrotic collagen and calcified matrix, which alter valve structure leading to inefficient opening of the valve and increased valvular pressure (21).

The VECs line both the ventricularis and fibrosa, serving as a protective layer of cells in the AV structure (22). Thus, VECs are also important for understanding the maintenance of a healthy functional valve and disease progression. In response to hemodynamic changes and proinflammatory cytokines, VECs, for instance, increase cell adhesion molecules such as intercellular adhesion molecule (ICAM) and vascular cellular molecule (VCAM) to promote the infiltration of monocytes and lymphocytes, which are essential components for tissue repair (17,22). Moreover, VECs regulate the phenotypic state of VICs via release of paracrine mediators. In a study using porcine valves, VECs secreted nitric oxide to reduce the differentiation of VICs to myofibroblasts and osteoblasts (23,24). These studies highlight the responsive and regulatory nature of VECs.

Comprising the most outer layer of the AV structure, VECs are in direct contact with blood flow and other hemodynamic-related stresses. Therefore, it is likely that VECs serve as signaling mediators and initiators of biological pathways in response to environmental stimuli (18). Past studies on vascular endothelial mechanotransduction provide insight into how VECs respond to hemodynamic stimuli and stressor, a process that is still not well understood (25). Studies by Shyy et al have revealed pathways involving displaced membrane integrins in VECs interacting with the extracellular matrix (ECM) and other cellular regulators at the basal membrane of the AV (26). Other studies show local strains due to flow stress in intermediate filaments within individual VECs as sensory detectors (27). Likewise, AV cytoskeleton, adhesion receptors, luminal membrane proteins, and ion channels were also implicated as being potential mechanotransducers, though more work is needed to fully understand the shear sensitive nature of both vascular and valvular endothelial cells (28).

1.3 Aortic Valve Calcification

Usually accompanied by other pathological characteristics, such as inflammation, lipid infiltration, thrombus formation, and fractured matrix fibers (29,30), AV calcification remains the most common cause of severe stenosis (31). Its progression is characterized by the thickening of the AV and formation of calcium nodules, which together are the first detectable cell structural changes in the leaflets (21). These pathological changes accumulate over time, eventually leading to reduced efficiency and function of the valve leaflets (10,21).

Interestingly, calcification of the AV is a side-dependent phenomenon (8), coinciding with different hemodynamic conditions on both sides of the AV (25,32,33) (Figure 2). For instance, calcification preferentially develops on the aortic face of the valve (fibrosa), which is mostly subjected to disturbed oscillatory blood flow, whereas the ventricular face (ventricularis), which is mostly subjected to stable laminar blood flow, remains relatively unaffected (33). The mechanisms responsible for this observed side-dependent AV calcification in the context of different local hemodynamic conditions remain unknown. Hence, our research objective is to discover mechanisms that can account for the observed differential side-dependent phenotypes between the fibrosa and ventricularis in differing hemodynamic conditions.

Early AV stenosis is associated with systemic endothelial dysfunction (34). In an *in situ* gene expression profile study involving porcine AVs, Simmons et al. discovered a differential down regulation of genes known to inhibit calcification in the endothelial cells on the fibrosa side compared to the ventricularis (35), suggesting the role VECs may play in the preferential calcification on the fibrosa in the AV. Moreover, our group has found that human aortic valvular endothelial cells (HAVECs) respond to shear stress due to blood flow by inducing changes in gene expression profiles (25). Specifically using HAVECs in our unique in vitro cone-and-plate

system to simulate different hemodynamic conditions in a preliminary study, we found significant differential expressions of several small nucleotide regulators known as microRNAs (miRNAs) between the fibrosa and ventricularis of the AV. Biological mechanisms involving endothelial miRNAs may play an important role in regulating AV homeostasis and calcification (25,36). Our lab's research aim is to study the role of mechanosensitive miRNAs in the differential response of HAVECs to disturbed flow.

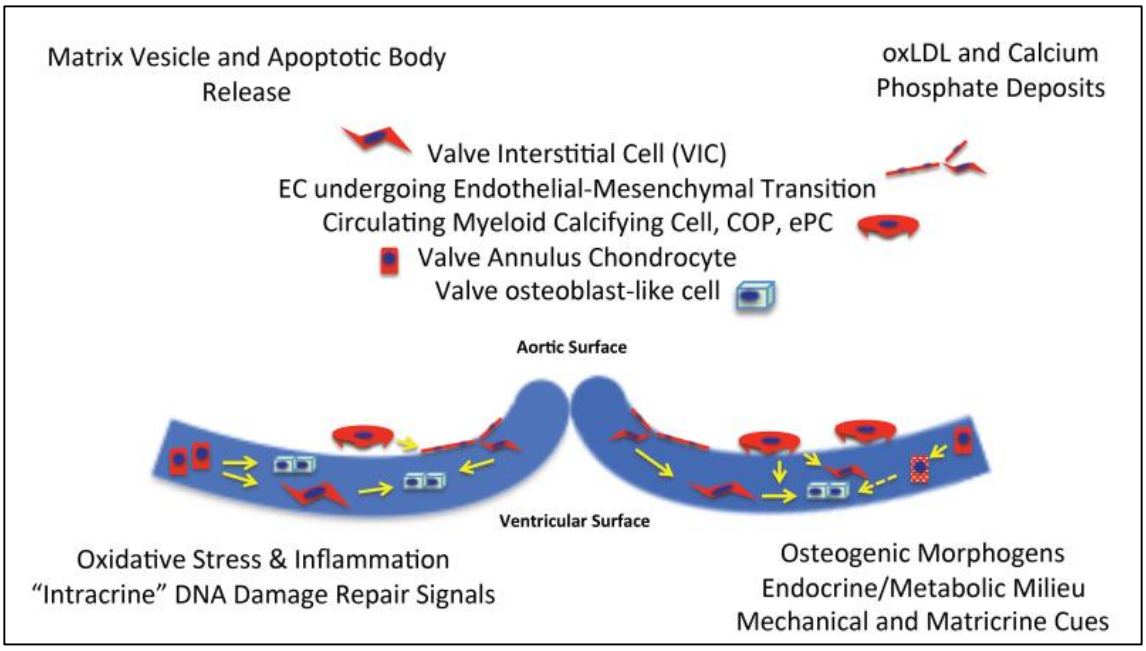

Figure 2. Calcification of the aortic valve. The AV is comprised of two surfaces: the fibrosa (facing the aorta) and ventricularis (facing the left ventricle). The AV is composed of endothelial cells lining the surface and valve interstitial cells within the AV. Moreover, the valve is constantly subjected to dynamic, environmental stimuli, which at times induce oxidative stress, inflammation, and endothelial-mesenchymal transition. Although the exact pathway for AV calcification remains unknown, many biological processes are involved in disease progression. Modified from (37).

1.4 Biogenesis of microRNAs

miRNAs are noncoding RNAs that post-transcriptionally regulate specific mRNAs by blocking protein translation and/or inducing mRNA degradation (38). There are several steps in the biogenesis of mature miRNAs (Figure 3). First, primary miRNA transcripts called pri-miRNAs are transcribed as individual miRNA genes, either from introns of protein-coding genes or polycistronic transcripts by RNA polymerase II. Typically several kilobases long with a cap and polyadenylated tail, pri-miRNAs fold into hairpin structures with imperfectly base-paired stems (39,40). Next, RNase-III enzyme Drosha processes the pri-miRNAs by cleaving the stem-loop structure, resulting in pre-miRNA structures that are 60-100 nucleotides long (40,41). After processing, pre-miRNAs are transported to the cytoplasm by nuclear transport receptors exportin (37,40,42). In the cytoplasm, RNase III Dicer cleaves pre-miRNAs into miRNA-miRNA duplexes of 18-22 nucleotides in length. Lastly, mature miRNAs are incorporated into the RNA-induced silencing complex (RISC), enabling specific post-translational gene regulation via translational repression and mRNA degradation (37).

With the capacity to fine-tune gene expression, miRNAs become key regulators of diverse biological and pathological processes, including development, apoptosis, cell proliferation and differentiation (43). Thus, dysregulation of miRNAs often result in impaired cell function and ultimately, disease progression (44). Based on our previous studies, these small non-coding RNAs may be key to understanding the intriguing phenomenon of preferential calcification on the fibrosa as opposed to the ventricularis.

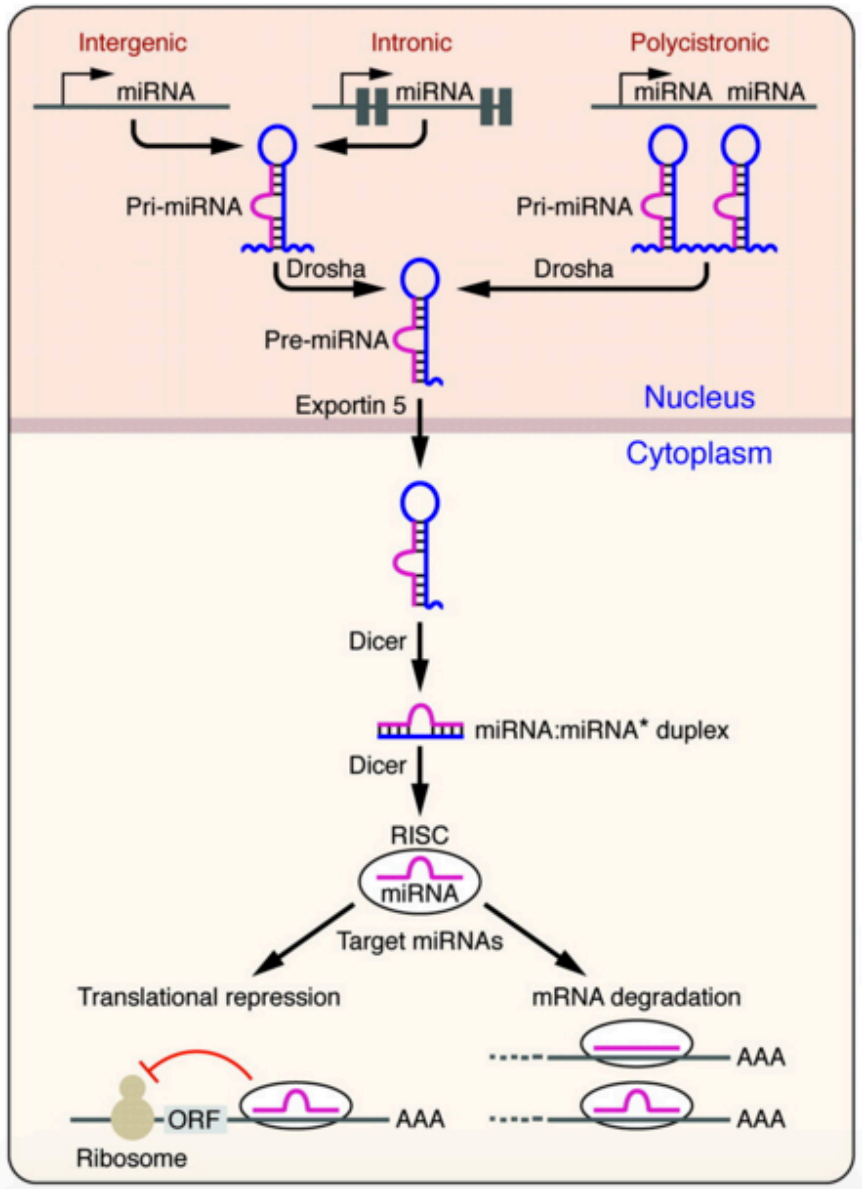

Figure 3. Schematic diagram of the miRNA biogenesis. Primary miRNA transcripts called pri-miRNAs are first transcribed as individual miRNA genes, either from introns of protein-coding genes or polycistronic transcripts by RNA polymerase II in the nucleus. pri-miRNAs fold into hairpin structures with imperfectly base-paired stems. Next, RNase-III enzyme Drosha processes pri-miRNAs, forming pre-miRNA structures, which after processing are transported to the cytoplasm by nuclear transport receptors exportin-5. Once in the cytoplasm, RNase III Dicer cleaves pre-miRNAs into miRNA-miRNA duplexes. Lastly, mature miRNAs are incorporated into the RNA-induced silencing complex (RISC), enabling specific post-translational gene regulation via translational repression and mRNA degradation. Modified from (45).

1.5 Foundational studies

In microarray studies by our group, we discovered a collection of potential shear – sensitive miRNA candidates based on their differential expressions in HAVECs subjected to laminar (LS) versus oscillatory shear (OS) (25). These findings are important because they build the foundation of our current work. In this study, we isolated HAVECs of both the fibrosa (F) and ventricularis (V) faces of the AV and subjected them to either LS or OS using our unique cone-and-plate system. After ECs were subjected to shear stress, their genetic profiles were mapped, shown in Figure 4. There were three main group analyses: FO vs. VL, the most physiological relevant group that is compared; FO vs. FL and VO vs. VL, which investigated the general shear-sensitive nature of both fibrosa and ventricularis endothelial cells (ECs) subjected to different stresses.

The objective of this thesis project is to confirm the shear-sensitivity of miRNAs discovered in these previous preliminary studies and study the roles they may play in side-dependent calcification. In preliminary findings, miRNA-181b has consistently demonstrated flow-sensitivity when comparing the genetic expression profiles of HAVECs subjected to LS and OS. Specifically, we observed relatively higher expression levels of miRNA-181b in HAVECs subjected to OS stress. With these findings, miRNA181b and its potential role in AV calcification will be the focus of this research.

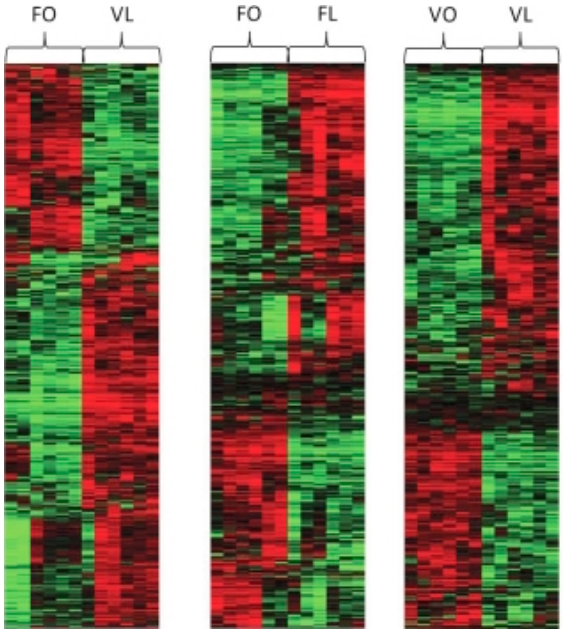

Figure 4. Differential expression profiles of HAVECs in response to LS vs OS. The microarray heat map compares the change of shear-sensitive genes in three main groups: FO versus VL, FO versus FL, and VO versus VL. Red shows upregulated genes and green shows down regulated genes. Modified from (25).

1.6 Objective of study

Located in chromosome 1 in humans, miRNA-181b is in proximity to multiple genes, including PTPRC, PEBP1P3, MIR181A1, MIR181A1HG, and RPS2P9, as shown in Figure 5. Sharing similar genetic sequences in chromosome 1, miRNA-181a and miRNA-181b are expressed near each other. Together, both miRNAs have been implicated in to play essential biological roles in retinal axon development and human immune cell differentiation, and they have been implicated as novel biomarkers for breast cancer cells (46-48).

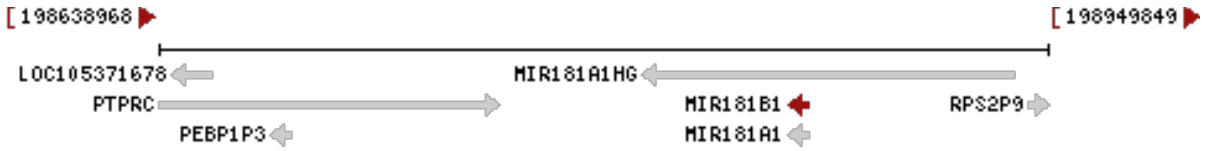

Figure 5. miRNA-181b Genomic Location. miRNA-181b is located in chromosome 1 at LOC105371678. It is located near PTPRC, PEBP1P3, MIR181A1, MIR181A1HG, and RPS2P9. (NCBI, http://www.ncbi.nlm.nih.gov/gene/406955).

miRNA-181b is important in a range of biological processes, including cancer-related apoptosis (49), tumor suppression (50) and cell growth (51). In the cardiovascular system, miRNA-181b plays an important role in vascular inflammation via NF-κB pathway (52), potentiation of EC differentiation from pluripotent human embryonic stem cells (53), and proliferation of vascular smooth muscle cells (54).

Moreover, using miRTarBase, an experimentally validated miRNA-target interaction database, we reviewed specific miRNA-181b targets, which included sirtuin-1 (SIRT1), GATA-binding protein 6 (GATA6), and tissue inhibitor of metallopeptidase 3 (TIMP3). Part of the sirtuin family, SIRT1 is a protein NAD+-dependent deacetylase that is most often localized in the nucleus and functions to regulate transcription factors epigenetically (55-57). GATA6 is also a transcription factor regulator and involved in biological processes, such as the regulation of cardiomyocyte hypertrophy (58) and embryonic development in mice studies (59), including healthy heart development (60). Lastly, TIMP3 targets and inhibits matrix metallopeptidases (MMPs) (61). MMPs are known to play an important role in ECM degradation (62). Because of its well-known role in diseases related to matrix degradation and its targeting by miRNA-181b, we will focus specifically on TIMP3 and its downstream target MMPs, as we consider a specific mechanism accounting for preferential AV calcification.

Timely maintenance and breakdown of the ECM are essential for embryonic development, morphogenesis, reproduction, and tissue remodeling (63). A family of >20 different MMPs degrade components of the ECM and play various roles in different physiological and pathological conditions, notably including cell migration (64). During early angiogenesis, ECs migrate into surrounding ECM, but in vitro studies demonstrated impairment of EC migration into collagen gels when MMP inhibitors were present (65). Moreover, studies have also demonstrated the importance of MMPs in wound healing; by using MMP inhibitors, Lund et al reduced keratinocyte migration and thus delayed wound healing in mice (66).

The endogenous inhibitor TIMP3 binds to MMPs in a 1:1 stoichiometry in a highly regulated process during development and tissue remodeling (61,67). Hence, TIMP3 expression levels have been studied in disease conditions involving changes in MMP activity. For example, in apolipoprotein E-deficient mice, adenovirus-mediated overexpression of TIMP3 reduces atherosclerotic lesions (68). In mice, TIMP3 deficiency disrupts matrix homeostasis and dilated cardiomyopathy (69). Moreover, foam cell macrophages, which are infiltrating inflammatory cells, were shown to exhibit both increased MMP-14 and decreased TIMP3 protein expression (70). With similar findings, Cardillim et al. also demonstrated significant reduction of TIMP3 in human carotid atherosclerotic plaques, correlated with high MMP-9 protein activity (71). In sum, these findings highlight the potential roles TIMP3 and MMPs may have in not only the maintenance of a healthy AV but also its disease progression.

Based on our preliminary studies, AV endothelial cells respond to stress by regulating shear-sensitive miRNAs, including miRNA-181b. miRNA-181b targets TIMP3, an inhibitor of the MMPs, leading to increased MMP activity and matrix degradation. Since calcification preferentially affects the AV fibrosa, the side that is subjected to OS, we predict greater MMP

activity for ECM breakdown in endothelial cells at the fibrosa versus the ventricularis. Therefore, **we hypothesize that miRNA181b is upregulated by disturbed flow at the AV fibrosa endothelium, leading to decreased expression of TIMP3 and increased matrix degradation.** The objective of this thesis is to investigate this novel biological mechanism responsible for side-dependent AV calcification and to discover novel therapeutic targets to attenuate or prevent the effects of differential environmental hemodynamic conditions in the AV.

Material and Methods

Cells and cell culture

Side-specific ventricularis HAVECs (vHAVECs) were isolated from non-calcified AVs obtained from heart transplant surgeries according to an Institutional Review Board-approved protocol at Emory University and Georgia Institute of Technology. The ECs were purified using Di-acetylated LDL and stored in a liquid nitrogen filled chamber, where the cells undergo induced dormancy.

Before subjecting the cells to shear stress, vHAVECs are first cultured in 12 mL plates with media comprised of shear medium (MCDB131), supplemented with 2.5% FBS, 1% L-glutamine, 1% penicillin-streptomycin. Each dish used to culture cells contains a thin layer of gelatin, which helps adhere ECs to the bottom plate surface. After vHAVECs establish confluency within 48 hours, we would next split the ECs into new 12 mL plates (n=8). During this step, vHAVECs were first washed with 10xPBS (Ambion, AM9625) and detached from the dish surface using Trypsin. The ECs were aliquotted equally into new dishes. Shear media were added to each plate, leaving a final total volume of 12 mL. The cells are ready to be subjected to shear stress via cone-and-plate system once the cells become confluent.

Shear stress using cone-and-plate system

After cells are cultured and become confluent, in vitro shear stress experiments were carried out using our cone-and-plate shears system, as shown in Figure 6. Laminar unidirectional shear stress was induced by parallel force of 20 dynes/cm^2, and disturbed flow, or oscillatory shear stress (OS) was induced at ± 5 dynes/cm^2, approximating the complex shear stress environment surrounding the aortic valve ECs (72). Further, the temperature of the reaction was set at 37 °C with 5% CO_2. After 24 hours, cell alignment, also as shown in Figure 6., was confirmed in LS and OS. Experiments were performed in quadruplicate.

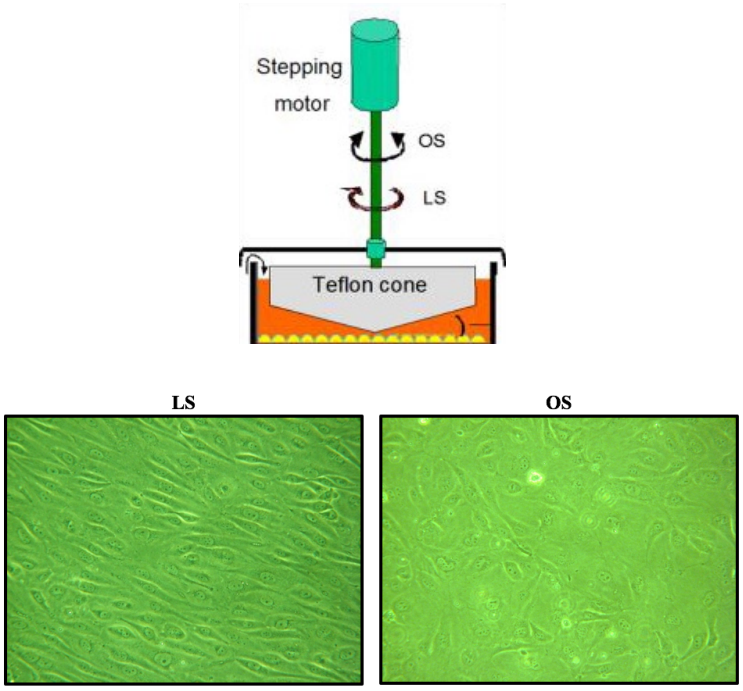

Figure 6. Cone-and-plate system and EC alignment by shear stress. Laminar unidirectional shear stress was induced by parallel force of 20 dynes/cm^2, and bidirectional oscillatory shear stress (OS) was induced at ± 5 dynes/cm^2, approximating the complex shear stress environment surrounding the aortic valve ECs. After 24 hours, cell alignment was confirmed. HAVECs subjected to LS stress demonstrate directional alignment, whereas cells subjected to OS stress aligned randomly.

Isolation of total RNA

After 24 hours of induced shear stress on vHAVECs using the cone-and-plate system, RNAs were extracted using procedures as defined in the Qiagen RNeasy kit. To begin the extraction process, vHAVECs were dissolved in 700 µL of QIAzol Lysis Reagent and homogenized using appropriate methods, in order to lyse and release EC RNA content. The homogenate was incubated at room temperature (15-25 °C) for 5 min. Next, 140 µL of chloroform was added to the sample and shaken vigorously for 15 s. After this homogenate was incubated at room temperature for 2-3 min, the sample was centrifuged for 15 min at 12,000 x g at 4 °C to encourage phase separation in the sample. The upper aqueous phase was transferred to a new collection tube, 1.5 volumes of 100% ethanol were added to precipitate RNA, and the sample was centrifuged at 8,000 x g for 15 s at room temperature. The membrane in the RNeasy Mini column was washed three times with 700 µL of Buffer RWT and dried via one more centrifugation. Finally, the RNA of the sample was collected in a new collection tube by dissolving in 30 µL of RNase-free water.

cDNA synthesis & quantitative Polymerase Chain Reaction (qPCR)

Using the collected RNAs as templates, cDNAs were generated for quantitative analysis. For cDNA based on miRNAs, we mixed 4 µL 5X miscript HiSpec buffer, 2 µL 10X miscript Nuclei mix, 2 µL miscript RT enzyme, and 2 µL RNase-free water with 10 µL isolated RNA. A reverse transcription reaction was performed via three steps in the Bio Rad thermal cycler: (1) 37 °C for 60 min; (2) 95 °C for 5 min; and (3) 4 °C, the optimal temperature for cDNA storage. For cDNA based on mRNAs, the sample mixture was comprised of 2 µL 10X buffer, 2 µL 10X random primers, 2 µL dNTP, 3 µL RNase-free water, and 1 µL transcriptase enzyme. Beginning

at 25°C for 10 min, the mRNA reverse transcriptase reaction was performed in three steps in the Bio Rad thermal cycler: (1) 37°C for 120 min; (2) 85°C for 5 min; (3) 4°C indefinitely.

PCR was conducted to amplify miRNA- and mRNA-based cDNAs using target primers. For miRNA-cDNAs, validated primers from Integrated DNA Technologies (IDT) or Qiagen were used to amplify DNA. The primers used are shown in the table below.

Gene	**Catalog Number**
199a-3p	81890353/IDT (ACAGTAGTCTGCACATTGGTTA)
214	81890355/ IDT (ACAGCAGGCACAGCAAGGCAGT)
181a	MS00008827/QIAGEN
181b	MS00006699/ QIAGEN
199-5p	MS00006741/ QIAGEN
U6	MS00033740/ QIAGEN

For mRNA-cDNAs, primers from previously published literature were used, shown in the table below.

	Primers (5'-3')		**Reference**
NLK	Forward	CCACTACCTTTATACCGAC	(73)
	Reverse	TACCTCGGAAACCACAACAG	
GATA6	Forward	ACCAGAGCCTAAACGCTTTC	(74)
	Reverse	ACCCTATCTCGGGATGCTAC	
CDX2	Forward	CAGTCGCTACATCACCATC	(75)
	Reverse	AGAGTCCACGCTCCTCAT	
TIMP3	Forward	CTACACCATCAAGCAGATGAAGATG	(76)
	Reverse	GCTCAGGGGTCTGTGGCATTGAT	
VSNL1	Forward	AAGTGATGGAGGACCTGGTG	(77)
	Reverse	GTCGCTCTTTGCAGCTTCTT	
BCL2	Forward	AAGCCGGCGACGACTTCT	(78)
	Reverse	GGTGCCGGTTCAGGTACTCA	
SIRT1	Forward	TGCTGGCCTAATAGAGTGGCA	(79)
	Reverse	CTCAGCGCCATGGAAAATGT	
18S	Forward	AGGAATTGACGGAAGGGCACCA	IDT
	Reverse	GTGCAGCCCCGGACATCTAAG	

For each target gene of interest, the sample mixture included 10 μL green SYBR mix, 1 μL of forward and reverse target primer, 7 μL DNase-free water, and 2 μL cDNA sample. For mi-RNA-based cDNA, we used U6 primers as control, and for mRNA-based cDNA, 18S target primers were used as control.

Using the Applied Biosystems, Inc., quantitative PCR system, we amplified target genes of interest as follows: samples were heated to 95°C, allowing for the activation HotStarTac DNA Polymerase. Next, for one cycle, there are three main steps: (1) DNA sample denatures into two separate strands for 15s at 94°C; (2) primers anneal to denatured DNA for 30 s at 55°C; and (3) the extension, or addition of complementary nucleotides, process proceeds for 30 s at 70°C, followed by fluorescence data collection. Thus, per one complete cycle, we amplify DNA by a factor of two. The exponential equation 2^n, where n is the number of complete cycles, calculates the total number of DNA strand that is created at the end of PCR cycles. Each DNA sample was set to complete 40 cycles. mRNA-based cDNAs were amplified using a similar protocol, with the DNA extension third step set for 1 min at 60°C. After all PCR cycles were completed, ΔC_T values were generated and analyzed.

Gelatinase Assay:

Using Life Technologies and Santa Cruz Biotechnology EnzChek kit, we measured extracellular matrix degradation using a gelatinase assay. The assay consisted of DQ gelatin fluorescein conjugate substrate, which is gelatin so heavily labeled with fluorescein that the fluorescence is quenched. When the gelatin substrate is exposed to enzymatic digestion, the assay yields high fluorescence intensity.

In our experiment, HAVECs were subjected to LS or OS stress in the cone-and-plate system, after which we isolated digestive enzymes using QIAzol. The collected enzyme samples were pipetted on to the gelatin substrate in the assay well. When the enzymes digest the gelatin, highly fluorescent fragments are released. When a sample yields high fluorescence intensity, we correlate the phenomenon with high digestive enzymatic activity and high extracellular matrix degradation. Using the fluorescence microplate reader, we measured the fluorescence intensity. Digestion products from the DQ gelatin substrate have absorption maxima at ~495 nm and fluorescence emission maxima at ~515 nm.

miRNA-181b Transfection

Using the Lipofectamine 2000 DNA Transfection kit, we treated HAVECs cells with pre- and anti-miRNA-181b at concentrations from 20 nM-100 nM. At the time of transfection, HAVECs were 70-90% confluent. In the process, we mixed the Lipofectamine reagent and pre- or anti-miRNA-181b in Opti-MEM medium, encouraging DNA-lipid complex formation for 5 min incubation at room temperature. Next, we added the DNA-lipid complex to the cell samples, transfecting the HAVECs. The cells were incubated at 37°C for 1-3 days and were analyzed as described above.

Statistics Analysis

Statistical analyses were performed using Excel. Error bars are reported as the standard deviation value. Pairwise comparisons were done using 2-tailed Student's *t* tests. Differences between groups were considered significant at $p < 0.05$, denoted * and $p < 0.01$, denoted **.

Results

LS/OS stress modulates miRNAs and target mRNA in HAVECs

To confirm the mechanical sensitivity of the miRNAs in our previous array, we subjected HAVECs to both LS and OS stresses using our cone-and-plate system and followed up with qPCR analyses to quantify genetic profile changes in HAVEC miRNAs and mRNAs. We found significant increase of miRNAs-181a and -181b expression in HAVECs exposed to OS versus those exposed to LS (Figure 7A). For both miRNAs-181a and -181b, the fold change increased approximately by a factor of 7 in OS conditions. These miRNAs were significantly and consistently observed to be the most mechanosensitive when compared to others found in the array, including miRNA-214, -199-3p, and -199-5p.

Based on the consistent increase in 181b in HAVECs and other endothelial cell types (25), we proceeded to study the HAVEC expression of miRNA-181b targets by quantifying the expression of predicted target mRNAs, again utilizing our cone-and-plate system and qPCR. First using miRTarBase, we compiled an *in silico* list of predicted 181b targets based on strongest evidence by validation methods. These potential targets included nemo-like kinase (NLK), GATA6, caudal type homeobox 2 (CDX2), TIMP3, SIRT1, visinin-like 1 VSNL1, and B-cell lymphoma 2 (BCL2) (Table 1). After subjecting HAVECs to LS or OS stress, we found genes GATA6, TIMP3, and SIRT1 were significantly downregulated in HAVECs exposed to OS compared to LS (Figure 7B). Other aforementioned genes were not significant and therefore not pursued further.

When juxtaposing both experiments, we observe significant upregulation of miRNA-181a and -181b in OS HAVECs along with significant correlational reduced expression of the predicted 181b targets GATA6, TIMP3, and SIRT genes. Because of its well-known role in

atherosclerosis, we further focused on TIMP3 and its effect on MMP activity in HAVECs under OS. In a valve tissue staining for TIMP3, we confirmed a higher and distinct expression of TIMP3 along the endothelial lining of the ventricularis compared to the fibrosa (Figure 7C).

Differential MMP activity and ECM degradation in LS/OS HAVECs

TIMP3 is a known inhibitor of MMPs and a key player in the initial steps leading to various phenotypic changes in endothelial cells (61). Therefore, we studied relative extracellular matrix degradation levels between LS and OS HAVECs to determine relative MMP activity after the cells were exposed to differential shear stresses. The fluorescent gelatinase assay has been shown to reflect cellular MMP levels by our group and others (80,81). In our experiment, HAVECs exposed to OS exhibited higher fluorescence signal at ~115 AU compared to LS (Figure 8A). This is correlated with higher MMP activity, or extracellular matrix degradation in OS HAVECs.

In addition to our *in vitro* MMP activity assay, we performed the gelatinase assay on human AV tissue, as we have previously shown (82). We observed a higher level of fluorescence in the fibrosa, subjected to OS, compared to the ventricularis, which is exposed to more LS conditions (Figure 8B). These findings were consistent with the results of the first gelatinase assay experiment, indicating relatively higher MMP and ECM degradation in the OS-subjected fibrosa and ECs than the LS-subjected ventricularis and ECs.

1.3 Validating TIMP3 as a miRNA-181b target

In our first experiments involving the cone-and-plate system and qPCR, we observed a correlation of three phenomena in OS: upregulation of miRNA-181b expression, downregulation

of the TIMP3 gene, and increased MMP activity. To show a direct relationship between miRNA-181b and TIMP3, we transfected HAVECs with pre-miRNA-181b using Lipofectamine to overexpress miRNA-181b and observe the effect on gene expression. First, we demonstrated with increasing concentration of pre-miRNA, expression of miRNA-181b also increased in HAVECS, indicating the efficacy of our pre-miRNA treatment method (Figure 9A). Moreover, in the pre-miRNA treated samples, the predicted target genes GATA6, TIMP3, and SIRT1 were significantly downregulated compared to the pre-miRNA control (Figure 9B). These three were, again, the only significantly altered target genes predicted from our in silico analysis.

To further validate the direct relationship of miRNA-181b as an inhibitory regulator of TIMP3, we treated HAVECs with anti-miR-181b to knockdown the miRNA-181b expression levels and also observe the effects on gene expression and MMP activity. First, we showed significantly reduced expression of miRNA-181b in HAVECS treated with anti-miRNA-181b compared to control samples, indicating efficacious transfection (Figure 10A). In the anti-miR-181b treated samples, we observed a significant decrease in fluorescent signal and therefore MMP activity compared to control samples. Thus, our study demonstrated in HAVECs treated with anti-miRNA-181b, MMP activity and ECM degradation also decreased.

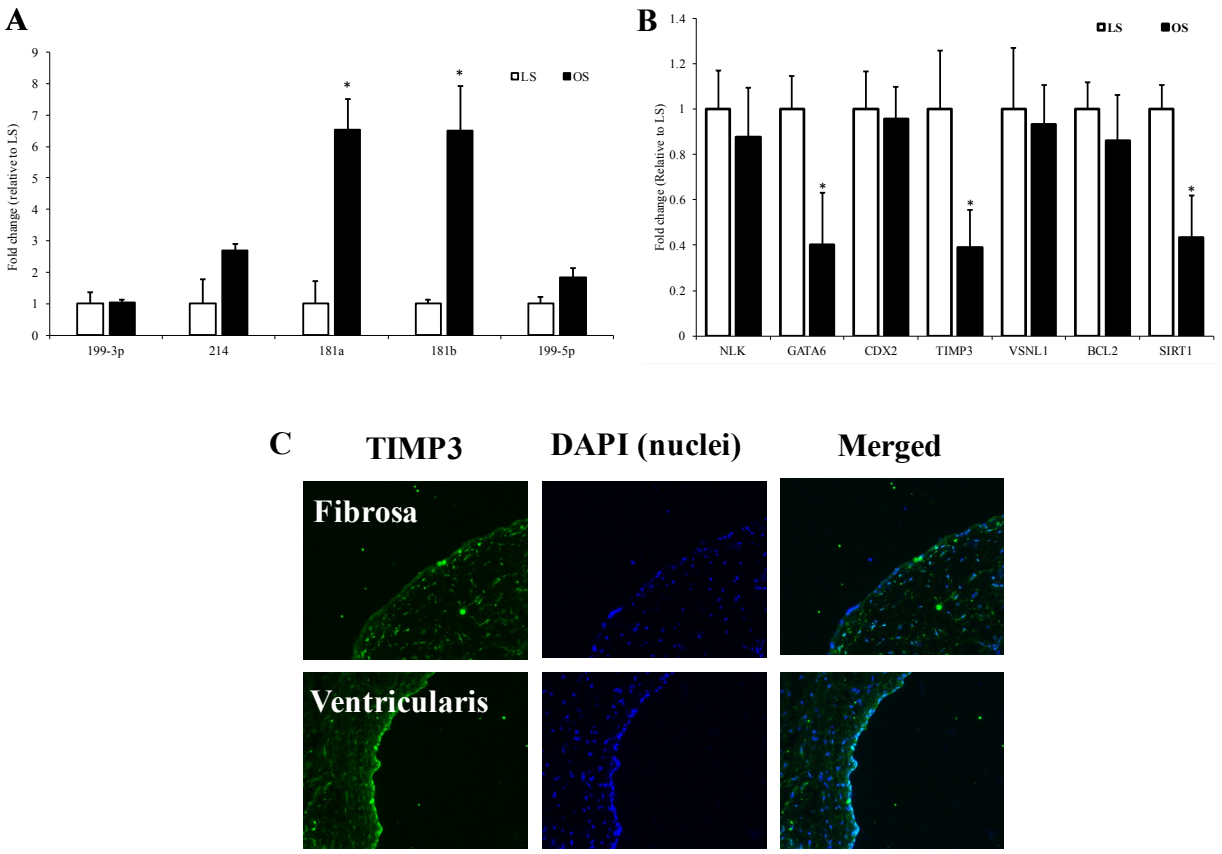

Figure 7. HAVEC miRNAs upregulated in oscillatory shear (OS) stress. HAVECs were subjected to LS or OS using the cone-and-plate viscometer for 24 hours. RNA was collected and real-time PCR was performed for both miRNA and mRNA expression. Valve tissues were further stained for TIMP3 protein expression. (a) miRNA-181a and -181b demonstrated significant and the greatest increase of fold change in HAVECs subjected to OS stress conditions compared to HAVECs in LS conditions. (b) Genes GATA6, TIMP3, and SIRT1 were significantly down regulated in OS HAVECs compared to LS HAVECs. (c) Valve tissue staining revealed higher TIMP3 expression along the endothelial lining of the AV ventricularis compared to the fibrosa.

		Validation methods						
		Strong evidence			Less strong evidence			
miRNA	Target	Reporter assay	Western blot	qPCR	Microarray	NGS	pSILAC	Other
hsa-miR-181b-5p	NLK	✔						✔
hsa-miR-181b-5p	GATA6	✔						✔
hsa-miR-181b-5p	CDX2	✔						✔
hsa-miR-181b-5p	TIMP3	✔	✔	✔				✔
hsa-miR-181b-5p	SIRT1	✔						
hsa-miR-181b-5p	VSNL1	✔		✔				✔
hsa-miR-181b-5p	BCL2	✔	✔	✔				✔

Table 1. miRTarBase miRNA-181b target predictions. miRTarBase, an experimentally validated miRNA-target interaction database, predicted miRNA-181b targets, including NLK, GATA6, CDX2, TIMP3, SIRT1, VSNL1, and BCL2, based on varying validation methods. In silico analysis indicated TIMP3 and BCL2 as miRNA-181b targets with strongest evidence. (Adapted from: http://mirtarbase.mbc.nctu.edu.tw/index.php).

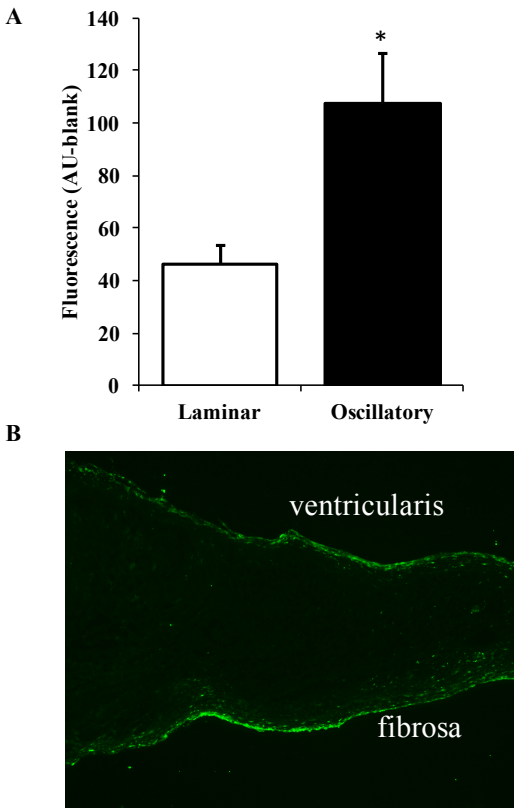

Figure 8. Gelatinase activity increase in OS stress. HAVECs were exposed to DQ gelatin fluorescein conjugate substrate to measure MMP activity. (a) HAVECs subjected to OS conditions indicated higher fluorescence signal compared to HAVECs subjected to LS conditions, indicating relatively higher MMP activity and greater extracellular matrix degradation in OS HAVECs. (b) Valve tissue staining demonstrated higher fluorescence intensity along the OS-subjected fibrosa than the LS-subjected ventricularis.

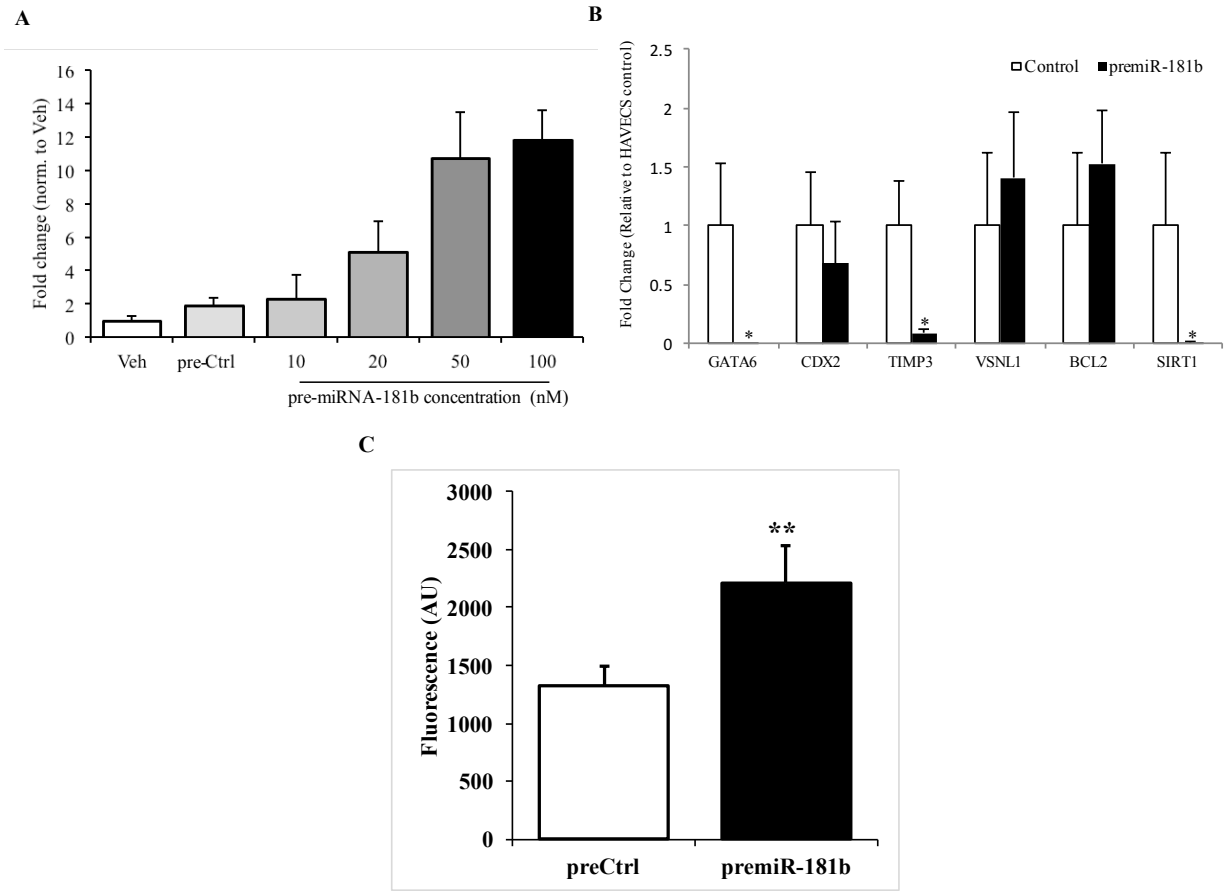

Figure 9. 181b targets predicted gene inhibiting of TIMP3. HAVECs were treated with pre-miR-181b, followed by real time qPCR. (a) Compared to control samples, the expression fold change of miRNA-181b increased along with increasing nM concentrations of pre-miRNA-181b in HAVECs. (b) In HAVECs treated with pre-miRNA-181b, genes GATA6, TIMP3, and SIRT1 were significantly downregulated compared to the control samples. (c) In the gelatinase assay, HAVECs treated with pre-miRNA-181b showed significantly higher fluorescence signal compared to control samples, indicating higher MMP activity and extracellular matrix degradation.

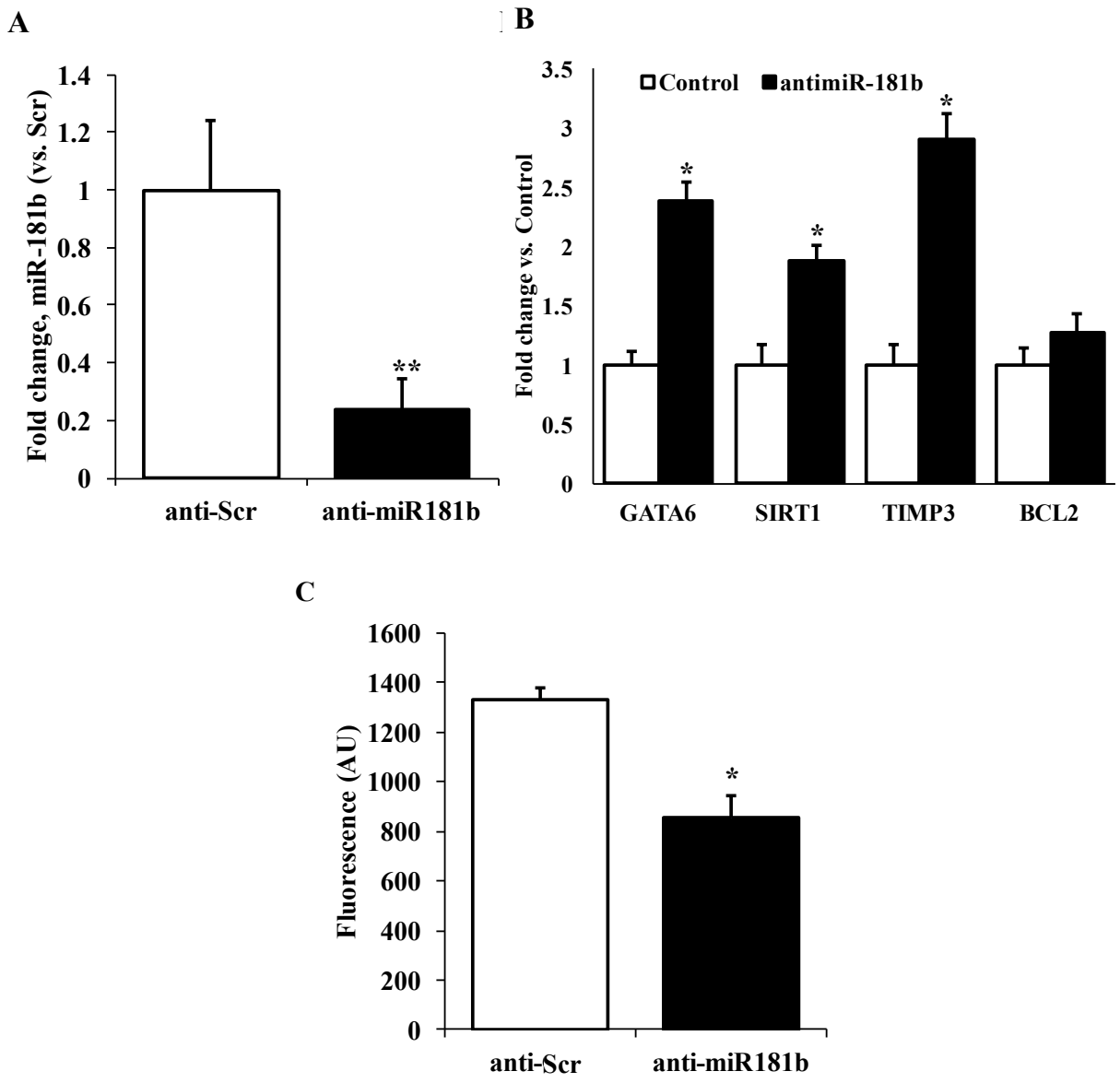

Figure 10. MMP activity after anti-miRNA-181b treatment in HAVECs. HAVECs were treated with anti-miRNA-181b and followed up with a gelatinase assay. (a) Compared to control samples treated with scrambled miRNAs, HAVECs treated with 50 nM anti-miRNA-181b showed significantly reduced expression of miRNA-181b. (b) Compared to control samples, HAVECs treated with anti-miRNA-181b showed significant increased expression of TIMP3. (c) In the gelatinase assay, HAVECs treated with anti-miRNA-181b showed significantly lower fluorescence signal compared to the control samples, indicating reduced MMP activity and extracellular matrix degradation.

Discussion

AV calcification is a side-dependent phenomenon. It mostly affects the OS-subjected fibrosa, whereas the ventricularis, which is subjected to LS, remains relatively unaffected (8,25,32,33). Using our unique cone-and-plate system followed by qPCR analyses, we simulated similar blood flow conditions, LS versus OS, in HAVECs to study a potential biological mechanism involving shear-sensitive miRNAs that can account for AV preferential calcification. The major findings of this study were significant correlational increase in miRNA-181b expression, decrease in TIMP3 expression, and increased MMP activity in HAVECs subjected to OS. These findings support our overall hypothesis: miRNA181b is upregulated by disturbed flow in the AV fibrosa endothelium, leading to decreased expression of TIMP3 and increased matrix degradation, summarized by Figure 11.

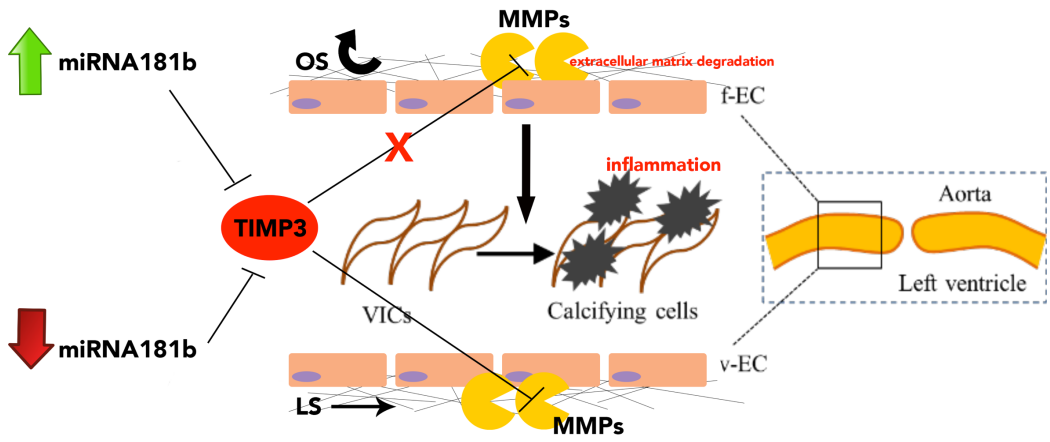

Figure 11. Proposed pathway mechanism in HAVECs. Ventricularis ECs are subjected LS stress, downregulating mechanosensitive miRNA-181b. Lowered expression of 181b leads to increased TIMP3 expression. The ventricularis therefore has relatively higher TIMP3 level, sequentially decreasing MMP activity responsible for ECM degradation. On the other hand, fibrosa ECs are subjected to OS stress, upregulating miRNA-181b. High levels of 181b reduce TIMP3 expression and therefore lead to higher levels of MMP activity and ECM degradation. With greater ECM degradation, inflammation results, and VICs transition into calcified cells.

In preliminary studies conducted by our lab, Holliday et al were amongst the first group to discover an array of mechanosensitive miRNAs in HAVECs of both fibrosa and ventricularis (25). From this pool of discovered miRNAs, we narrowed and identified specific shear-sensitive miRNAs, including miRNA-181a, -181b, -214, -199-3p, and -199-5p, to further study. Here, we confirmed the mechanosensitive nature of and found significant upregulation of miRNA-181a and -181b in HAVECs subjected to OS stress (Figure 7A). Other aforementioned miRNAs did not significantly change between HAVECs subjected to LS or OS stress and therefore were not further studied. Although preliminary studies predicted these miRNAs as being shear-sensitive, the discrepancy between array and our results could be explained by the fact that our in vitro experiments were more controlled compared to the preliminary study, which utilized cells of differing patient sources. Hence, ECs of differing patient sources may have responded to induced shear stress differently. In the validation studies shown here, we used endothelial cells from only one patient source, reducing potential extraneous factors that might have affected the array.

Of 181a and 181b, we chose to further study 181b because of its known role in atherosclerosis. Atherosclerosis is also a progressive disease of the large arteries and is characterized by the accumulation of lipids and fibers (83). CAVD is an early progressive disease, often beginning with AV sclerosis lesions that are similar to early atherosclerotic plaques but eventually progress toward severe calcification and stenosis (1,10). In previous studies using apolipoprotein E-deficient mice, systemic delivery of miRNA-181b inhibited the NF-κB pathway and atherosclerosis via cell-specific mechanisms in the valvular endothelium (52,84). Interestingly, although that study showed the therapeutic advantage of miRNA-181b in reducing inflammation, we observed relatively and significantly higher expression of miRNA-181b in HAVECs subjected to OS. A possible explanation for the discrepancy between the

former study and ours includes the intrinsic differences between human ECs and those of mice (85). Moreover, the former study also focused on vascular endothelial cell, whereas our study utilized cells derived from the aortic valve. Butcher et al. showed important differences in the response of these two cell populations to shear stress and inflammatory stimuli (86). Both facts highlight different cell sources as important potential causes for the differences we have observed in the valvular endothelium.

We next focused on miRNA-181b targets, also using the cone-and-plate system and qPCR. First, we performed an in silico analysis of miRNA-181b using miRTarBase to compile a list of interesting 181b targets based on validation methods and evidence strength. These targets included NLK, GATA6, CDX2, TIMP3, SIRT1, VSNL1, and BCL2 (Table 1). Our findings showed significant down regulation of SIRT1, GATA6, and TIMP3 mRNA expression in HAVECs subjected to OS stress (Figure 7B). From the three genes, we chose to further study TIMP3 because of its known role as an inhibitor for MMPs and thus important regulators of extracellular matrix degradation (61,62). Hence, we performed a valve tissue staining for TIMP3 expression and observed a relatively higher and distinct expression of TIMP3 along the endothelial lining of the ventricularis compared to the fibrosa (Figure 7C). The results from this tissue staining confirmed our previous findings, since the ventricularis is subjected to LS. Similar to the findings from Figure 7A and 7B, we expected the ventricularis to exhibit downregulation of miRNA-181b and thus has relatively higher expression of TIMP3.

SIRT1 and GATA6 are also interesting miRNA-181b targets because of their roles as transcription factors regulators in biological processes, including development and cell apoptosis (55-60). During cardiac hypertrophy, SIRT1 upregulated the activity of the histone variant H2A.Z, resulting in its ubiquitin-mediated degradation and thus consequential modulation of cell

growth and apoptosis (87,88). Moreover, in other studies, SIRT1 deficient mice often died from cardiac defects (88,89), underlining the important role that SIRT1 may have in cardiac function. Similarly, GATA6 and GATA4 expression were critical for normal cardiac development and when deficient, were lethal in mice development (90,91). Overall, their roles as transcription factor regulators implicate epigenetic level regulation that may also be involved with preferential AV calcification. However, additional studies must first be performed before constructing any definitive conclusion. In our future studies, we would follow up with a similar research approach for the SIRT1 and GATA6 genes, as we have performed for TIMP3 and MMP. Since both seemed to be implicated in epigenetics, for instance, it would be interesting to investigate how the knockout of genes SIRT1 and GATA6 change the gene expression profile of HAVECs using microarrays.

Since miRNA-181b is upregulated in OS (Figure 7A) and predictively targets TIMP3, which we have shown to decrease in OS condition (Figure 7B), we predicted an increase in MMP activity in HAVECs subjected to OS stress. Interestingly, MMP activity is considered a proximal biomarker for cardiac remodeling and a distal biomarker for inflammation (92). Since our data showed significant down regulation of TIMP3 in HAVECs subjected to OS, we predicted an increased MMP activity in the ECs, in turn, underlining the essential role extracellular matrix degradation may play in calcification on the AV fibrosa. Using a fluorescein substrate-based gelatinase assay, we found a higher fluorescent signal in HAVECs subjected to OS than LS (Figure 8A). As far as we know, this is also the first attempt using the gelatinase assay to measure and study MMP activity in the valvular endothelium. We correlate high fluorescence with high enzymatic activity or MMP activity and ECM degradation. Thus, HAVECs subjected to OS condition exhibited greater ECM degradation than LS. Moreover, we

also showed higher fluorescent signal along the endothelial lining of the AV fibrosa compared to the ventricularis (Figure 8B). This result supports our first gelatinase assay finding because the AV fibrosa is subjected to OS and thus, as we predicted, should exhibit higher fluorescence and ECM degradation.

Thus far, we have demonstrated three significant phenomena in HAVECs subjected to OS stress: 1) upregulation of miRNA-181b, 2) decreased expression of TIMP3, and 3) increased MMP activity. These findings are however only correlational. To show a direct relationship between miRNA-181b and TIMP3, we first transfected HAVECs with pre-miRNA-181b using Lipofectamine to overexpress miRNA-181b and observe the effect on gene expression. First, we demonstrated with increasing concentrations of pre-miRNA-181b treatment, miRNA-181b expression also increased in HAVECs, confirming the efficacy of our transfection methods (Figure 9A). Next, we found in pre-miRNA treated HAVECs, the predicted target genes GATA6, TIMP3, and SIRT1 were significantly downregulated compared to the pre-miRNA control (Figure 9B). These genes were again the only significantly altered targets in OS condition from our first cone-and-plate and qPCR study (Figure 7B). Further, in our gelatinase assay, we showed HAVECS treated with pre-miRNA-181b demonstrated higher fluorescence compared to control samples, therefore indicating higher levels of ECM degradation and MMP activity (Figure 9C).

Moreover, we transfected HAVECs with anti-mir181b to knockdown 181b expression and observe the effects on gene expression. We first demonstrated in HAVECs that were treated with anti-miRNA-181b, miRNA-181b was significantly reduced compared to control samples, again showing effective transfection in HAVECs (Figure 10A). After HAVECs were treated with anti-miRNA-181b, we proceeded to perform qPCR, showing significantly increased

expression of TIMP3, as well in GATA6 and SIRT1 (Figure 10B). In our followed up gelatinase assay, we observed significant decrease in fluorescent signal for HAVECs treated with anti-miRNA-181b compared to control samples (Figure 10C). Again, we correlate the reduced fluorescence signal in HAVECs sampled to reduced MMP activity and ECM degradation. Thus, we demonstrated with anti-miRNA-181b, MMP activity also decreased. Though these observed correlations are most probable due to the regulation of TIMP3, we must first conduct additional future directional studies confirming the direct, regulatory relationship between TIMP3 and MMPs before constructing definitive conclusions. Moreover, our next step in future studies includes studying HAVECs after pre- and anti-miRNA181b transfection in dynamic conditions by our cone-and-plate system and to expand our model to ex vivo studies using porcine valves, which better encompasses the complex tissue.

In summary, we identified shear-sensitive miRNA-181b and studied its targets to understand a potential biological mechanism for the intriguing phenomenon of AV preferential calcification. Here, we propose one of the first mechanisms that attempts to link preferential calcification to differing hemodynamic conditions of the AV via mechanosensitive miRNAs. Our study also further provides insight on the role endothelial cells play in the development of CAVD. Although there are many biological processes involved in the progression of AV calcification, our study attempts to elucidate one specific biological process of the complex disease pathway. Moreover, as targets of miRNA-181b and because of their known roles in ECM degradation, we also identified TIMP3 and its target MMPs as potential therapeutic targets of AV disease. In the future, these targets, particularly anti-miRNA-181b, may become the first noninvasive treatment options, particularly anti-miRNA-181b, for patients who are affected by AV calcification and other cardiovascular diseases.

References

1. Bossé Y, Mathieu P, Pibarot P. Genomics: The Next Step to Elucidate the Etiology of Calcific Aortic Valve Stenosis. Journal of the American College of Cardiology 2008;51:1327-1336.

2. Nkomo VT, Gardin JM, Skelton TN, Gottdiener JS, Scott CG, Enriquez-Sarano M. Burden of valvular heart diseases: a population-based study. The Lancet;368:1005-1011.

3. Faggiano P, Antonini-Canterin F, Baldessin F, Lorusso R, D'Aloia A, Cas LD. Epidemiology and cardiovascular risk factors of aortic stenosis. Cardiovascular Ultrasound 2006;4:27-27.

4. LlNDROOS M, KUPARI M, VALVANNE J, STRANDBERG T, HEIKKILÄ J, TlLVIS R. Factors associated with calcific aortic valve degeneration in the elderly. European Heart Journal 1994;15:865-870.

5. Mohler ER, Nichols R, Harvey WP, Sheridan MJ, Waller BF, Waller BF. Development and progression of aortic valve stenosis: Atherosclerosis risk factors—a causal relationship? a clinical morphologic study. Clinical Cardiology 1991;14:995-999.

6. Otto CM, Lind BK, Kitzman DW, Gersh BJ, Siscovick DS. Association of Aortic-Valve Sclerosis with Cardiovascular Mortality and Morbidity in the Elderly. New England Journal of Medicine 1999;341:142-147.

7. Stewart BF, Siscovick D, Lind BK et al. Clinical Factors Associated With Calcific Aortic Valve Disease fn1. Journal of the American College of Cardiology 1997;29:630-634.

8. Mohler Iii ER. Mechanisms of aortic valve calcification. The American Journal of Cardiology 2004;94:1396-1402.

9. Mozaffarian D, Benjamin EJ, Go AS et al. Heart Disease and Stroke Statistics—2015 Update: A Report From the American Heart Association. Circulation 2014.

10. Freeman RV, Otto CM. Spectrum of Calcific Aortic Valve Disease: Pathogenesis, Disease Progression, and Treatment Strategies. Circulation 2005;111:3316-3326.

11. Roger VL, Go AS, Lloyd-Jones DM et al. Heart Disease and Stroke Statistics—2011 Update: A Report From the American Heart Association. Circulation 2011;123:e18-e209.

12. Otto CM. Timing of aortic valve surgery. Heart 2000;84:211-218.

13. Chester AH, El-Hamamsy I, Butcher JT, Latif N, Bertazzo S, Yacoub MH. The living aortic valve: From molecules to function. Global Cardiology Science & Practice 2014;2014:52-77.

14. Esmerats JF, Heath; J, Hanjoong J. Shear-Sensitive Genes in Aortic Valve Endothelium Antioxidants & Redox Signaling 2016;00.

15. Chen J-H, Simmons CA. Cell–Matrix Interactions in the Pathobiology of Calcific Aortic Valve Disease: Critical Roles for Matricellular, Matricrine, and Matrix Mechanics Cues. Circulation Research 2011;108:1510-1524.

16. Schoen FJ. Evolving Concepts of Cardiac Valve Dynamics: The Continuum of Development, Functional Structure, Pathobiology, and Tissue Engineering. Circulation 2008;118:1864-1880.

17. Wang H, Leinwand LA, Anseth KS. Cardiac valve cells and their microenvironment[mdash]insights from in vitro studies. Nat Rev Cardiol 2014;11:715-727.

18. Butcher JT, Penrod AM, García AJ, Nerem RM. Unique Morphology and Focal Adhesion Development of Valvular Endothelial Cells in Static and Fluid Flow Environments. Arteriosclerosis, Thrombosis, and Vascular Biology 2004;24:1429-1434.

19. Liu AC, Joag VR, Gotlieb AI. The Emerging Role of Valve Interstitial Cell Phenotypes in Regulating Heart Valve Pathobiology. The American Journal of Pathology 2007;171:1407-1418.

20. Osman L, Yacoub MH, Latif N, Amrani M, Chester AH. Role of Human Valve Interstitial Cells in Valve Calcification and Their Response to Atorvastatin. Circulation 2006;114:I-547-I-552.

21. Rajamannan NM, Evans FJ, Aikawa E et al. Calcific Aortic Valve Disease: Not Simply a Degenerative Process: A Review and Agenda for Research From the National Heart and Lung and Blood Institute Aortic Stenosis Working GroupExecutive Summary: Calcific Aortic Valve Disease – 2011 Update. Circulation 2011;124:1783-1791.

22. Butcher JT, Nerem RM. Valvular endothelial cells and the mechanoregulation of valvular pathology. Philosophical Transactions of the Royal Society of London B: Biological Sciences 2007;362:1445-1457.

23. Gould ST, Matherly EE, Smith JN, Heistad DD, Anseth KS. The role of valvular endothelial cell paracrine signaling and matrix elasticity on valvular interstitial cell activation. Biomaterials 2014;35:3596-3606.

24. Richards J, El-Hamamsy I, Chen S et al. Side-Specific Endothelial-Dependent Regulation of Aortic Valve Calcification: Interplay of Hemodynamics and Nitric Oxide Signaling. The American Journal of Pathology 2013;182:1922-1931.

25. Holliday CJ, Ankeny RF, Jo H, Nerem RM. Discovery of shear- and side-specific mRNAs and miRNAs in human aortic valvular endothelial cells. American Journal of Physiology - Heart and Circulatory Physiology 2011;301:H856-H867.

26. Shyy JY-J, Chien S. Role of Integrins in Endothelial Mechanosensing of Shear Stress. Circulation Research 2002;91:769-775.

27. Helmke BP, Thakker DB, Goldman RD, Davies PF. Spatiotemporal Analysis of Flow-Induced Intermediate Filament Displacement in Living Endothelial Cells. Biophysical Journal 2001;80:184-194.

28. Hahn C, Schwartz MA. Mechanotransduction in vascular physiology and atherogenesis. Nat Rev Mol Cell Biol 2009;10:53-62.

29. Otto CM. Calcification of bicuspid aortic valves. Heart 2002;88:321-322.

30. Thiene G, Basso C. Pathology and pathogenesis of infective endocarditis in native heart valves. Cardiovascular Pathology 2006;15:256-263.

31. Lloyd-Jones D, Adams RJ, Brown TM et al. Heart Disease and Stroke Statistics—2010 Update: A Report From the American Heart Association. Circulation 2010;121:e46-e215.

32. Otto CM, Kuusisto J, Reichenbach DD, Gown AM, O'Brien KD. Characterization of the early lesion of 'degenerative' valvular aortic stenosis. Histological and immunohistochemical studies. Circulation 1994;90:844-53.

33. Weinberg EJ, Mack PJ, Schoen FJ, García-Cardeña G, Kaazempur Mofrad MR. Hemodynamic Environments from Opposing Sides of Human Aortic Valve Leaflets Evoke Distinct Endothelial Phenotypes In Vitro. Cardiovascular Engineering (Dordrecht, Netherlands) 2010;10:5-11.

34. Poggianti E, Venneri L, Chubuchny V, Jambrik Z, Baroncini LA, Picano E. Aortic valve sclerosis is associatedwith systemic endothelial dysfunction. Journal of the American College of Cardiology 2003;41:136-141.

35. Simmons CA, Grant GR, Manduchi E, Davies PF. Spatial Heterogeneity of Endothelial Phenotypes Correlates With Side-Specific Vulnerability to Calcification in Normal Porcine Aortic Valves. Circulation research 2005;96:792-799.

36. Kumar S, Kim CW, Son DJ, Ni CW, Jo H. Flow-dependent regulation of genome-wide mRNA and microRNA expression in endothelial cells in vivo. Scientific Data 2014;1:140039.

37. van Rooij E. The Art of MicroRNA Research. Circulation Research 2011;108:219-234.

38. Ambros V. The functions of animal microRNAs. Nature 2004;431:350-355.

39. CAI X, HAGEDORN CH, CULLEN BR. Human microRNAs are processed from capped, polyadenylated transcripts that can also function as mRNAs. RNA 2004;10:1957-1966.

40. Ha M, Kim VN. Regulation of microRNA biogenesis. Nat Rev Mol Cell Biol 2014;15:509-524.

41. Lee Y, Ahn C, Han J et al. The nuclear RNase III Drosha initiates microRNA processing. Nature 2003;425:415-419.

42. Yi R, Qin Y, Macara IG, Cullen BR. Exportin-5 mediates the nuclear export of pre-microRNAs and short hairpin RNAs. Genes & Development 2003;17:3011-3016.

43. Goettsch C, Hutcheson JD, Aikawa E. MicroRNA in Cardiovascular Calcification: Focus on Targets and Extracellular Vesicle Delivery Mechanisms. Circulation Research 2013;112:1073-1084.

44. Bartel DP. MicroRNAs: Target Recognition and Regulatory Functions. Cell;136:215-233.

45. Towler DA. Molecular and Cellular Aspects of Calcific Aortic Valve Disease. Circulation research 2013;113:198-208.

46. Bisso A, Faleschini M, Zampa F et al. Oncogenic miR-181a/b affect the DNA damage response in aggressive breast cancer. Cell Cycle 2013;12:1679-1687.

47. Carrella S, Barbato S, D' Agostino Y et al. TGF-β Controls miR-181/ERK Regulatory Network during Retinal Axon Specification and Growth. PloS one 2015;10:e0144129.

48. Presnell SR, Al-Attar A, Cichocki F, Miller JS, Lutz CT. Human Natural Killer Cell microRNA: Differential Expression of MIR181A1B1 and MIR181A2B2 Genes Encoding Identical Mature microRNAs. Genes and immunity 2015;16:89-98.

49. Li D, Jian W, Wei C et al. Down-regulation of miR-181b promotes apoptosis by targeting CYLD in thyroid papillary cancer. International Journal of Clinical and Experimental Pathology 2014;7:7672-7680.

50. Shi Z-m, Wang X-f, Qian X et al. MiRNA-181b suppresses IGF-1R and functions as a tumor suppressor gene in gliomas. RNA 2013;19:552-560.

51. Xia Y, Gao Y. MicroRNA-181b promotes ovarian cancer cell growth and invasion by targeting LATS2. Biochemical and Biophysical Research Communications 2014;447:446-451.

52. Sun X, Icli B, Wara AK et al. MicroRNA-181b regulates NF-κ B–mediated vascular inflammation. The Journal of Clinical Investigation 2012;122:1973-1990.

53. Kane NM, Howard L, Descamps B et al. Role of MicroRNAs 99b, 181a, and 181b in the Differentiation of Human Embryonic Stem Cells to Vascular Endothelial Cells. Stem Cells (Dayton, Ohio) 2012;30:643-654.

54. Li T-J, Chen Y-L, Gua C-J, Xue S-J, Ma S-M, Li X-D. MicroRNA 181b promotes vascular smooth muscle cells proliferation through activation of PI3K and MAPK pathways. International Journal of Clinical and Experimental Pathology 2015;8:10375-10384.

55. Chang H-C, Guarente L. SIRT1 and other sirtuins in metabolism. Trends in Endocrinology & Metabolism;25:138-145.

56. Michan S, Sinclair D. Sirtuins in mammals: insights into their biological function. The Biochemical journal 2007;404:1-13.

57. Rahman S, Islam R. Mammalian Sirt1: insights on its biological functions. Cell Communication and Signaling 2011;9:1-8.

58. Liang Q, De Windt LJ, Witt SA, Kimball TR, Markham BE, Molkentin JD. The Transcription Factors GATA4 and GATA6 Regulate Cardiomyocyte Hypertrophy in Vitro and in Vivo. Journal of Biological Chemistry 2001;276:30245-30253.

59. Koutsourakis M, Langeveld A, Patient R, Beddington R, Grosveld F. The transcription factor GATA6 is essential for early extraembryonic development. Development 1999;126:723-732.

60. Molkentin JD, Antos C, Mercer B, Taigen T, Miano JM, Olson EN. Direct Activation of a GATA6 Cardiac Enhancer by Nkx2.5: Evidence for a Reinforcing Regulatory Network of Nkx2.5 and GATA Transcription Factors in the Developing Heart. Developmental Biology 2000;217:301-309.

61. Brew K, Dinakarpandian D, Nagase H. Tissue inhibitors of metalloproteinases: evolution, structure and function1. Biochimica et Biophysica Acta (BBA) - Protein Structure and Molecular Enzymology 2000;1477:267-283.

62. Nagase H, Visse R, Murphy G. Structure and function of matrix metalloproteinases and TIMPs. Cardiovascular Research 2006;69:562-573.

63. Nagase H, Woessner JF. Matrix Metalloproteinases. Journal of Biological Chemistry 1999;274:21491-21494.

64. Vu TH, Werb Z. Matrix metalloproteinases: effectors of development and normal physiology. Genes & Development 2000;14:2123-2133.

65. Fisher C, Gilbertson-Beadling S, Powers EA, Petzold G, Poorman R, Mitchell MA. Interstitial Collagenase Is Required for Angiogenesis in Vitro. Developmental Biology 1994;162:499-510.

66. Lund LR, Romer J, Bugge TH et al. Functional overlap between two classes of matrix-degrading proteases in wound healing. The EMBO Journal 1999;18:4645-4656.

67. Visse R, Nagase H. Matrix Metalloproteinases and Tissue Inhibitors of Metalloproteinases: Structure, Function, and Biochemistry. Circulation Research 2003;92:827-839.

68. Rouis M, Adamy C, Duverger N et al. Adenovirus-Mediated Overexpression of Tissue Inhibitor of Metalloproteinase-1 Reduces Atherosclerotic Lesions in Apolipoprotein E–Deficient Mice. Circulation 1999;100:533-540.

69. Fedak PWM, Smookler DS, Kassiri Z et al. TIMP-3 Deficiency Leads to Dilated Cardiomyopathy. Circulation 2004;110:2401-2409.

70. Johnson JL, Jenkins NP, Huang W-C et al. Relationship of MMP-14 and TIMP-3 Expression with Macrophage Activation and Human Atherosclerotic Plaque Vulnerability. Mediators of Inflammation 2014;2014:276457.

71. Cardellini M, Menghini R, Martelli E et al. TIMP3 Is Reduced in Atherosclerotic Plaques From Subjects With Type 2 Diabetes and Increased by SirT1. Diabetes 2009;58:2396-2401.

72. Sucosky P, Balachandran K, Elhammali A, Jo H, Yoganathan AP. Altered Shear Stress Stimulates Upregulation of Endothelial VCAM-1 and ICAM-1 in a BMP-4– and TGF- β 1–Dependent Pathway. Arteriosclerosis, Thrombosis, and Vascular Biology 2009;29:254-260.

73. Cichocki F, Felices M, McCullar V et al. miR-181 promotes human NK cell development by regulating Notch signaling. Journal of immunology (Baltimore, Md : 1950) 2011;187:6171-6175.

74. Li C, Li X, Pang S et al. Novel and Functional DNA Sequence Variants within the GATA6 Gene Promoter in Ventricular Septal Defects. International Journal of Molecular Sciences 2014;15:12677-12687.

75. Sritanaudomchai H, Sparman M, Tachibana M et al. CDX2 in the Formation of the Trophectoderm Lineage in Primate Embryos. Developmental biology 2009;335:179-187.

76. Gu P, Xing X, Tänzer M et al. Frequent Loss of TIMP-3 Expression in Progression of Esophageal and Gastric Adenocarcinomas. Neoplasia (New York, NY) 2008;10:563-572.

77. Williams TA, Monticone S, Crudo V, Warth R, Veglio F, Mulatero P. Visinin-Like 1 Is Upregulated in Aldosterone-Producing Adenomas With KCNJ5 Mutations and Protects From Calcium-Induced Apoptosis. Hypertension 2012;59:833-839.

78. Briton-Jones C, Lok IH, Po ALS, Cheung CK, Chiu TTY, Haines C. Changes in the ratio of Bax and Bcl-2 mRNA expression and their cellular localization throughout the ovulatory cycle in the human oviduct. Journal of Assisted Reproduction and Genetics 2006;23:149-156.

79. Chen X, Sun K, Jiao S et al. High levels of SIRT1 expression enhance tumorigenesis and associate with a poor prognosis of colorectal carcinoma patients. Scientific Reports 2014;4:7481.

80. Krejner A, Grzela T. Modulation of matrix metalloproteinases MMP-2 and MMP-9 activity by hydrofiber-foam hybrid dressing – relevant support in the treatment of chronic wounds. Central-European Journal of Immunology 2015;40:391-394.

81. Mazzoni A, Nascimento FD, Carrilho M et al. MMP Activity in the Hybrid Layer Detected with in situ Zymography. Journal of Dental Research 2012;91:467-472.

82. Son DJ, Kumar S, Takabe W et al. The atypical mechanosensitive microRNA-712 derived from pre-ribosomal RNA induces endothelial inflammation and atherosclerosis. Nature communications 2013;4:3000-3000.

83. Lusis AJ. Atherosclerosis. Nature 2000;407:233-241.

84. Sun X, He S, Wara AKM et al. Systemic Delivery of MicroRNA-181b Inhibits Nuclear Factor- κ B Activation, Vascular Inflammation, and Atherosclerosis in Apolipoprotein E–Deficient Mice. Circulation Research 2014;114:32-40.

85. Mestas J, Hughes CCW. Of Mice and Not Men: Differences between Mouse and Human Immunology. The Journal of Immunology 2004;172:2731-2738.

86. Butcher JT, Tressel S, Johnson T et al. Transcriptional Profiles of Valvular and Vascular Endothelial Cells Reveal Phenotypic Differences: Influence of Shear Stress. Arteriosclerosis, Thrombosis, and Vascular Biology 2006;26:69-77.

87. Chen I-Y, Lypowy J, Pain J et al. Histone H2A.z Is Essential for Cardiac Myocyte Hypertrophy but Opposed by Silent Information Regulator 2 α . Journal of Biological Chemistry 2006;281:19369-19377.

88. Lavu S, Boss O, Elliott PJ, Lambert PD. Sirtuins [mdash] novel therapeutic targets to treat age-associated diseases. Nat Rev Drug Discov 2008;7:841-853.

89. Cheng H-L, Mostoslavsky R, Saito Si et al. Developmental defects and p53 hyperacetylation in Sir2 homolog (SIRT1)-deficient mice. Proceedings of the National Academy of Sciences 2003;100:10794-10799.

90. Maitra M, Schluterman MK, Nichols HA et al. Interaction of Gata4 and Gata6 with Tbx5 is critical for normal cardiac development. Developmental biology 2009;326:368-377.

91. Xin M, Davis CA, Molkentin JD et al. A threshold of GATA4 and GATA6 expression is required for cardiovascular development. Proceedings of the National Academy of Sciences 2006;103:11189-11194.

92. Halade GV, Jin Y-F, Lindsey ML. Matrix Metalloproteinase (MMP)-9: a proximal biomarker for cardiac remodeling and a distal biomarker for inflammation. Pharmacology & therapeutics 2013;139:32-40.